9

INJURY BIOMECHANICS RESEARCH
Proceedings of the Thirty-Third International Workshop

Finite Element Model Simulation of Airbag-Dummy Interaction

Z. Lu and P. Chan

ABSTRACT

This paper reports a validation of a finite element airbag-dummy model and a study of airbag-dummy interaction. The airbag model is constructed using LS-Ingrid software and integrated with the LSTC Hybrid III dummy models with the simulations performed using LS-DYNA. Simulations have been carried out using two airbags and two dummy sizes. Validation against laboratory out-of-position (OOP) data shows good data agreement with airbag pressure and dummy kinematics while only qualitative agreement is observed for neck load data comparison. The model captures the key events of airbag deployment and loading. Simulation studies of the effects of dummy standoff and crash speed on dummy responses have been completed with reasonable results obtained.

INTRODUCTION

Airbags are effective supplemental restraint systems for occupant protection in automobile collisions. Research and advances are ongoing in improving the effectiveness of the airbag in reducing the hazards to small occupants in out-of-position (OOP) situations (Patrick and Nyquist, 1972; Lau et al., 1993; Yoganandan et al., 1993; Johnston et al., 1997) without compromising the crash protection for large occupants. To reduce airbag-induced injuries, the requirements and criteria for low risk airbag deployment are mandated in the FMVSS 208 in the US (NHTSA, 2000).

The study of airbag-occupant interaction problems has primarily depended on dummy testing, but mathematics-based computer simulations are needed to provide scientific understanding with theoretical framework in parallel with testing. Finite element (FE) simulation has great potential to fulfill the analytical need for detailed understanding of the airbag-dummy interaction dynamics. In the past decade, some airbag studies have been carried out with finite element simulations (O'Connor and Rao, 1992; Wawa et al., 1993; Ruan and Prasad, 1994; Lin et al., 1995; Diggies et al., 1997; Tanavde et al., 1997; Plank et al., 1998; Vaidyaraman et al., 1998; Sieveka et al., 1999; Petit et al., 2003) but model validation with detailed data comparison is very much lacking. In idealized crash simulations the airbag is usually predeployed with the dummy moving into the airbag. However, in OOP situations with the occupant in close proximity, the occupant interacts with the airbag inflation right in the beginning where the bag unfolding process and gas flow effects are important, requiring a complex and difficult modeling treatment. Issues of gas dynamics effects, airbag folding complexities, and dummy modeling are challenges to using finite element models for airbag studies.

The objective of this paper is to develop and validate an integrated finite element model for the study of airbag-dummy interaction. The finite element airbag models have been previously developed and validated against data obtained from airbag deployment against cylindrical surrogate targets (Lu and Chan, 2005). The validated airbag models have been integrated with the 5th and 50th percentile Hybrid III dummy models available from LSTC. Simulations have been performed to validate the integrated models against dummy test data. Parametric simulations under static and crash conditions have also been carried out to study the effects of proximity and crash speed on airbag load and dummy responses. The present work provides an evaluation of the currently available Hybrid III dummy models for airbag load studies.

METHODS

Test Data

The selected benchmark data for model validation are obtained from previous Airbag Test Simulator (ATS) tests. As shown in Figure 1, the ATS is a pneumatically driven test apparatus that can be calibrated to replicate the inflation of fleet airbags (Bandak et al., 2002; Lu and Chan, 2003). Using a controlled release from a pressurized reservoir prefilled by compressed gas, the ATS can be used to inflate airbags for impact tests without using fleet inflators. It has been shown that the ATS data have a high degree of repeatability, which is especially suitable for model validation purposes.

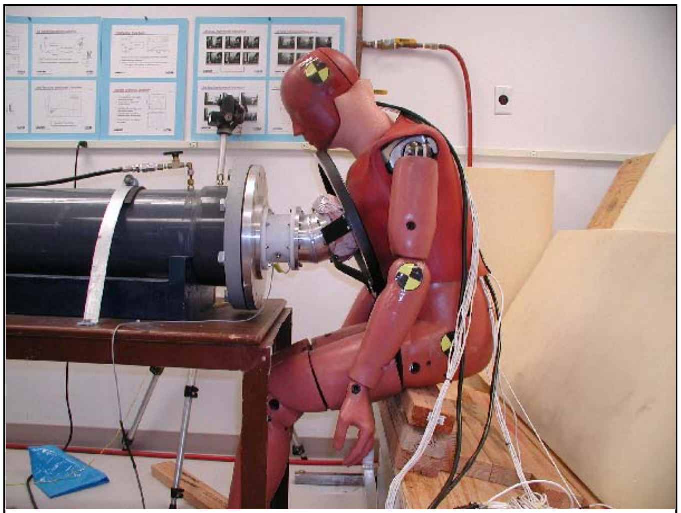

Figure 1: ATS apparatus and Hybrid III dummy.

Two fleet driver-side airbags, A and B, one from a minivan and the other from a mid-size sedan, were used in the ATS impact tests. Sealed tank tests conforming to the SAE J2238 standard recorded peak pressures of 207 and 152 KPa for the inflators from bags A and B, respectively. Both bags are composed of two assembled circular pieces of silicon-coated airbag fabric with two vent holes on the rear fabric piece. Bag A has an accordion folding pattern while bag B has a reverse-roll folding pattern. The diameter of the flattened bag is 686 mm for bag A and 660 mm for bag B. However, bag A has smaller leak holes (25 mm) than bag B (38 mm). Due to its stronger inflator and smaller leak holes, bag A exerts much stronger loading on the dummy.

Finite Element Model

In OOP situations, the occupant interacts with the airbag at the early stage of bag deployment. Bag design parameters like the cover tear pattern and bag folding can affect the bag inflation process. An OOP simulation needs to start from a folded bag and model the entire bag inflation and occupant interaction. Using the LS-Ingrid software, the folded models for bag A and bag B were constructed from meshed airbag geometry CAD files. The details and physical properties of the FE bag models were previously described by Lu and Chan (2005).

The FE models for bag A and bag B have been previously validated against the ATS test data for free swinging cylindrical surrogate targets (Lu and Chan, 2005). Two cylindrical targets of different sizes were used in the ATS tests with the target standoff from the airbag varied over a range from in-position (IP) to out-of-position (OOP) proximities. The calculated bag pressures and target responses were shown to agree well with the data (Lu and Chan, 2005).

In the current study, the previously validated airbag model is placed inside a chamber, which serves as the base and backing for the bag deployment. The chamber can be covered with a bag cover to simulate the whole airbag module. Alternatively, the cover can be removed to simulate deployments without bag cover. The chamber is connected to spokes and the steering wheel to complete the airbag-steering wheel module (Figure 2a). The steering wheel has a diameter of 370 mm - the same as that used in the ATS tests. The chamber, spoke, and steering wheel are modeled as a rigid body.

For dummy simulations, the deformable 5th and 50th Hybrid III models from LSTC were used (Figure 2b). LSTC has provided the Hybrid III models for users but their validation status is not known. The LSTC deformable dummy model is a combination of some deformable parts and many rigid components, which contains a deformable neck and a deformable chest rib cage, as well as the rigid head skull and rigid spine. Simulations were carried out with the airbag-steering wheel model placed in front of the dummy model in the ISO-2 OOP situation - the same as the test configuration (Figure 2b). A general purpose type 5 (NODES_TO_SURFACE) contact was used for the bag fabric-to-dummy contact algorithm. The interface friction coefficient was 0.1.

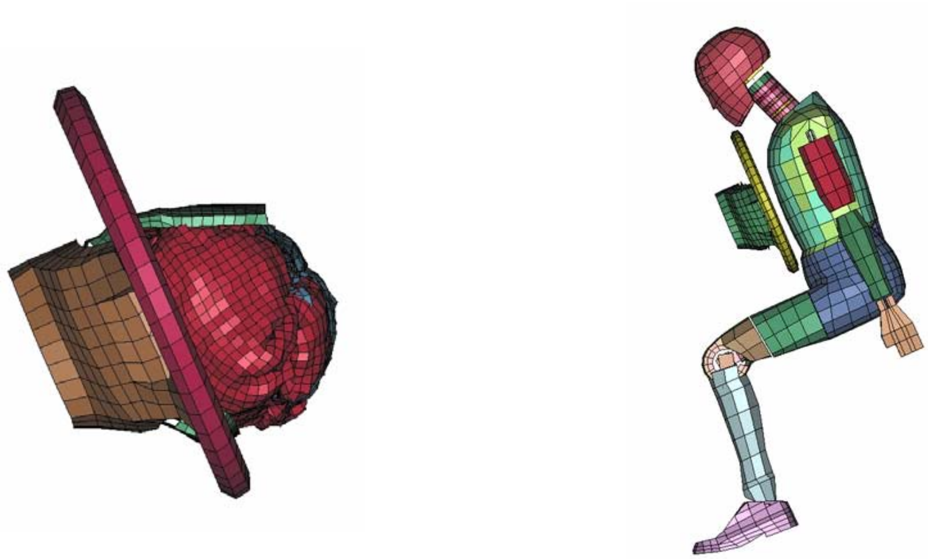

(a) Airbag-steering wheel module with airbag partially inflated

(b) Airbag-steering wheel module in front of dummy

Figure 2: Airbag-steering wheel and dummy model.

The FE software used for this study was LS-DYNA, and the uniform pressure gas-flow option was selected. The airbag was inflated by specifying the mass flow rate and gas temperature. The inflator mass flow rate and gas temperature for each airbag module were derived from the sealed tank test and the ATS inflation data (Bandak et al., 2002).

RESULTS

Model Validation

For the 50th percentile dummy model, a limited validation of the dummy head/neck response against the Naval Biodynamics Laboratory (NBDL) sled test data (Seemann et al., 1986) was first carried out. The 15-g –X sled test (with no impact) was used for the present validation. All dummy components below the first thoracic vertebral body (T1) were set to be rigid in the model. The recorded horizontal acceleration was applied to the T1 vertebra to drive the model and the calculated head rotation response was compared against data. The simulated dummy head/neck response is in good agreement with the NBDL test results for the head rotation, angular velocity and acceleration (Figure 3). This result shows the head/neck model produces reasonable rotational kinematics data agreement with the historical benchmark data.

Four ISO-2 airbag tests were simulated using the integrated airbag-dummy models (Figure 2b): (1) 5th percentile dummy with bag A, (2) 5th percentile dummy with bag B, (3) 50th percentile dummy with bag A, and (4) 50th percentile dummy with bag B. The airbag pressure and dummy kinematics data comparison are presented first followed by neck load data comparison.

The calculated airbag pressures agree with the ATS measurements fairly well for all four configurations (Figures 4a, 5a, 6a, and 7a). The initial punch-out, intermediate over-expansion, and final pressurization phases are well captured by the finite element simulations. For the initial punch-out (0-10 ms) and final pressurization (30-60 ms) phases, the simulation results match the measurements especially well. Overall, the calculated airbag pressures for the 5th percentile dummy agree with data better than for the 50th percentile dummy (Figures 4a vs. 6a and 5a vs. 7a).

The calculated head accelerations agree with the ATS measurements reasonably well for all cases (Figures 4b, 5b, 6b, and 7b). For bag A, the calculated head accelerations do not have the initial pulse around 10 ms in contrast to the data (Figures 4b and 6b). The calculated acceleration is higher than the data from 30-80 ms for bag B with the 5th percentile dummy (Figure 5b). The simulations capture the trend that for the same dummy, the peak head acceleration for the stronger bag A is about twice as that for the weaker bag B (Figures 4b vs. 5b and 6b vs. 7b). Overall, the timing and trend of the calculated head accelerations are very similar to the data (Figures 4b, 5b, 6b, and 7b).

The calculated chest accelerations also agree with the ATS measurements well (Figures 4c, 5c, 6c, and 7c). The chest acceleration data for the 5th percentile dummy show some spikes during the initial punch-out phase around 10 ms (Figures 4c and 5c), which are not found in the 50th percentile dummy data (Figures 6c and 7c). The 5th percentile dummy data also show a late-time spike between 75-90 ms that is not due to the airbag interaction but more likely a data acquisition anomaly (Figures 4c and 5c).

For bag A with the 5th percentile dummy, the calculated airbag contact load is compared against the dummy contact load derived from inverse dynamics based on the dummy kinematics data. At the ISO-2 position, the dummy chest is in direct contact with the airbag module at the beginning, which exerts a high load on the chest (Figure 1). The FE simulation also shows the airbag load on the chest is much higher than that on the head and neck (Figure 8a). The airbag also applies a strong initial punch-out load on the dummy chest from 3 to 13 ms (Figure 8a).

Since there was no chest rotational data for full kinematics reconstruction, two different methods were employed to simplify and solve the inverse dynamics problem: (1) assume the upper torso rotates about a stationary hip joint, and (2) assume negligible rotational effects. The high-speed movie shows that the dummy motion is somewhere between these two assumptions; i.e., there is some torso rotation about the hip that also has some translation. Therefore, these two methods would predict the low and high limits of the airbag-chest contact forces. Figure 8b shows the favorable contact force data comparison for the test using bag A with the 5th percentile dummy, giving additional validation of the contact force calculation method implemented in the LS-DYNA model. The oscillations in the inverse dynamics calculations from 3 to 15 ms (Figure 8b) are due to the oscillations in the chest acceleration data (Figure 4c).

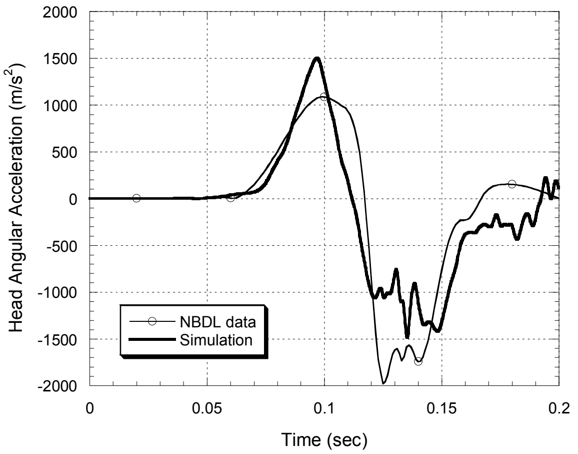

(a) Head angular acceleration

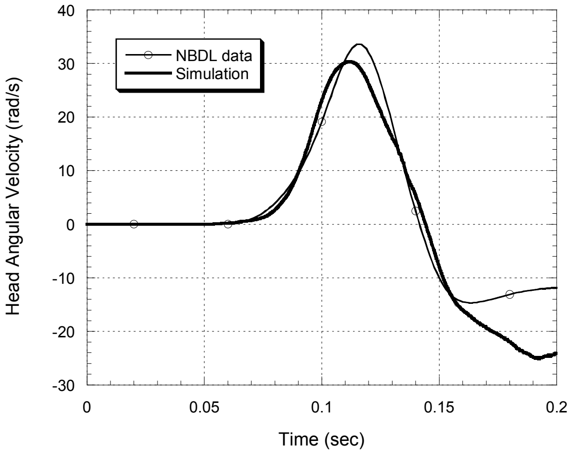

(b) Head angular velocity

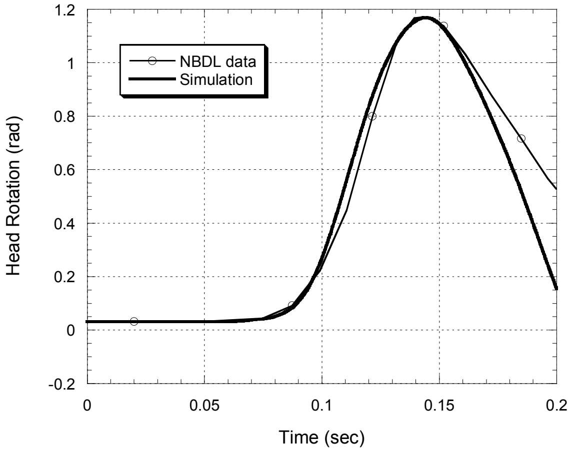

(c) Head rotation

Figure 3: Validation of Hybrid III dummy model against NBDL sled test data.

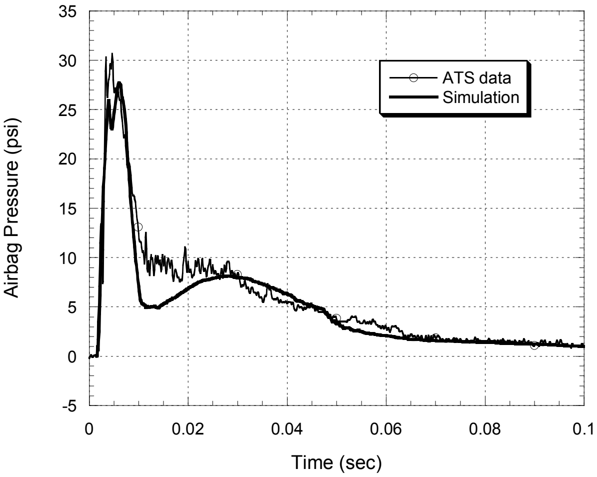

(a) Airbag pressure

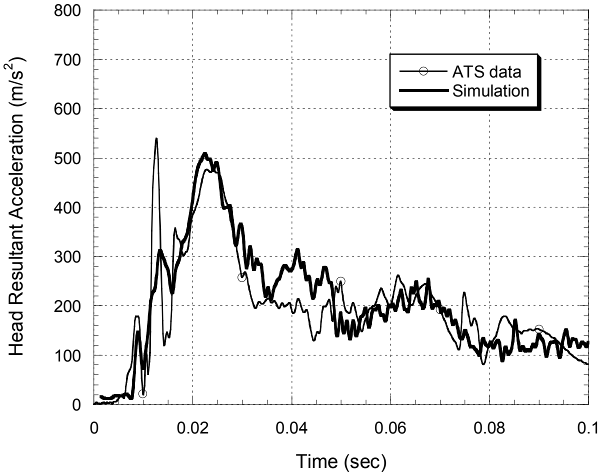

(b) Head acceleration

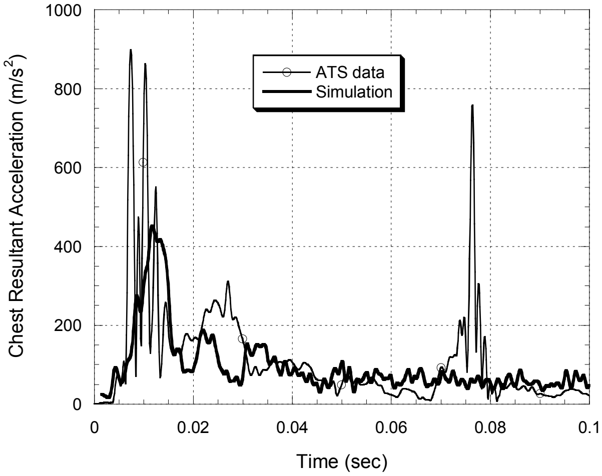

(c) Chest acceleration

Figure 4: Validation of bag A with 5th percentile dummy model.

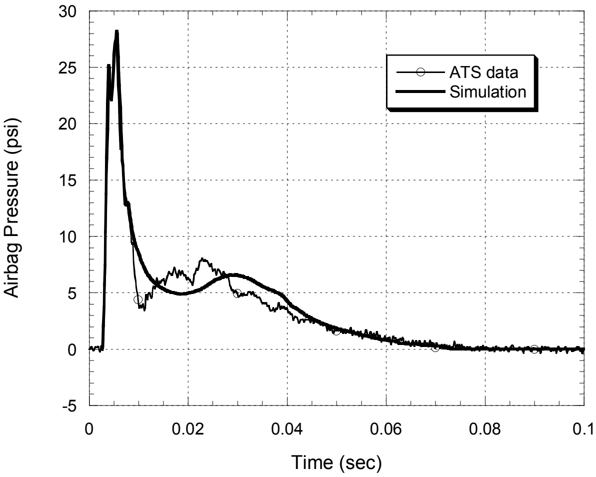

(a) Airbag pressure

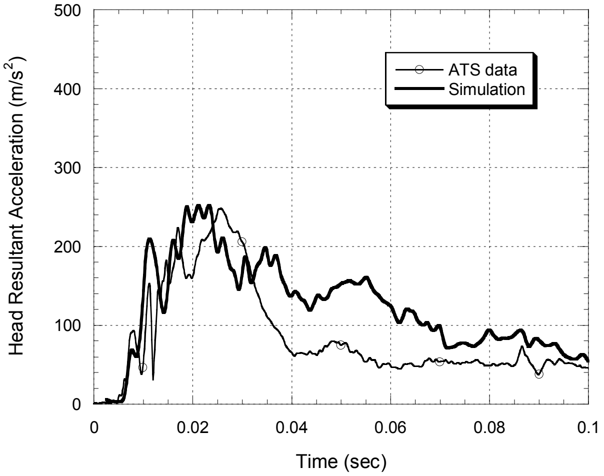

(b) Head acceleration

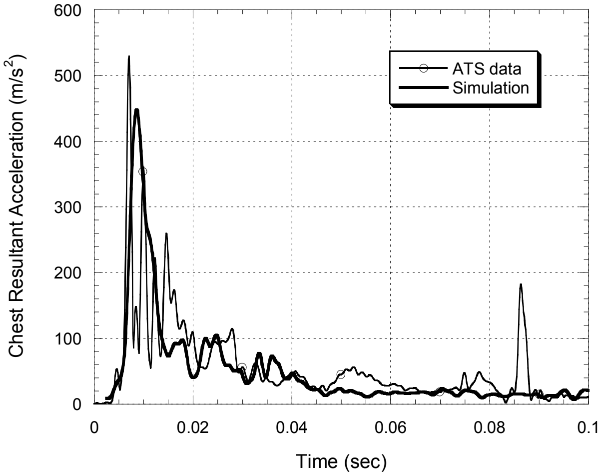

(c) Chest acceleration

Figure 5: Validation of bag B with 5th percentile dummy model.

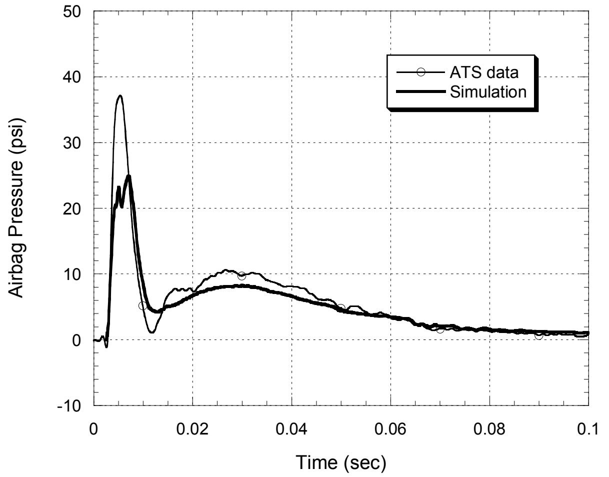

(a) Airbag pressure

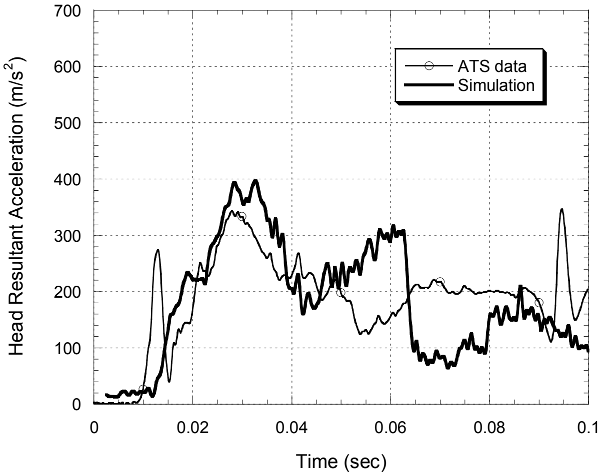

(b) Head acceleration

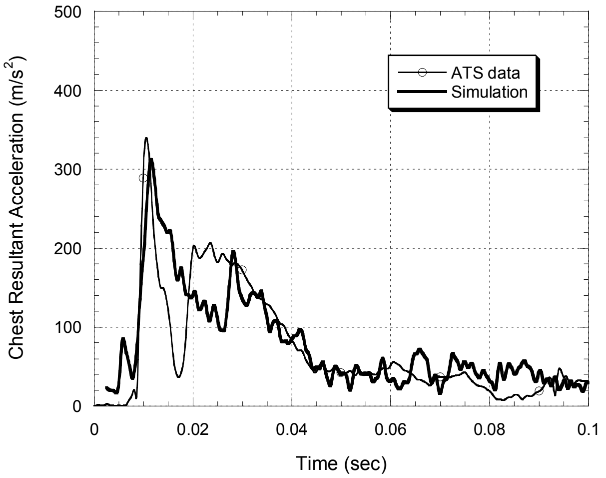

(c) Chest acceleration

Figure 6: Validation of bag A with 50th percentile dummy model.

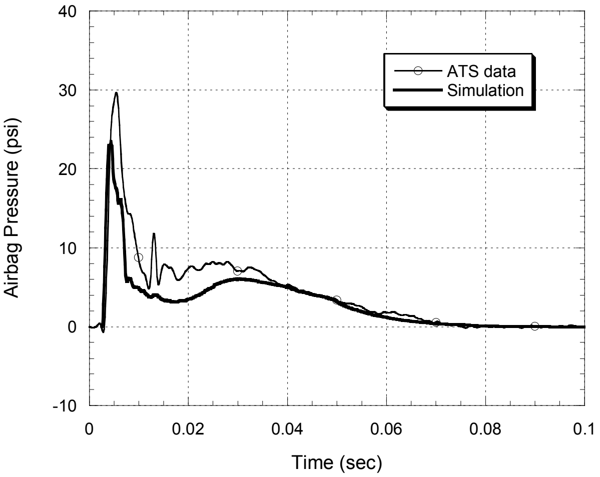

(a) Airbag pressure

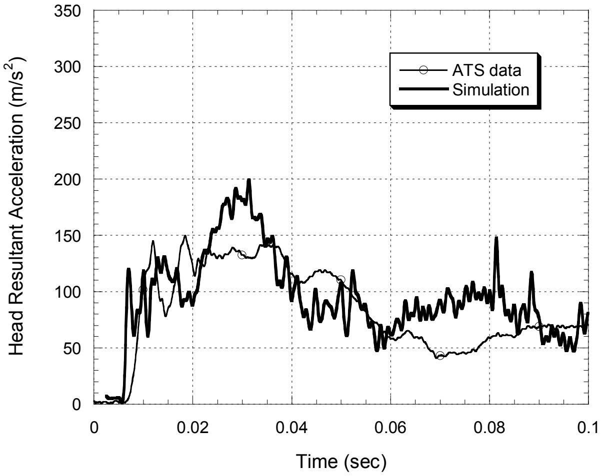

(b) Head acceleration

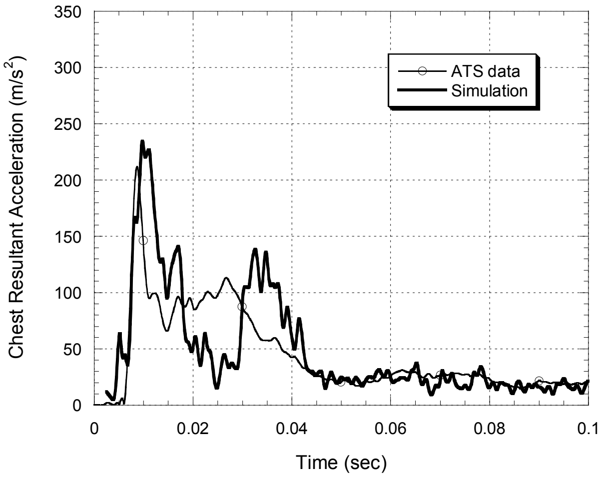

(c) Chest acceleration

Figure 7: Validation of bag B with 50th percentile dummy model.

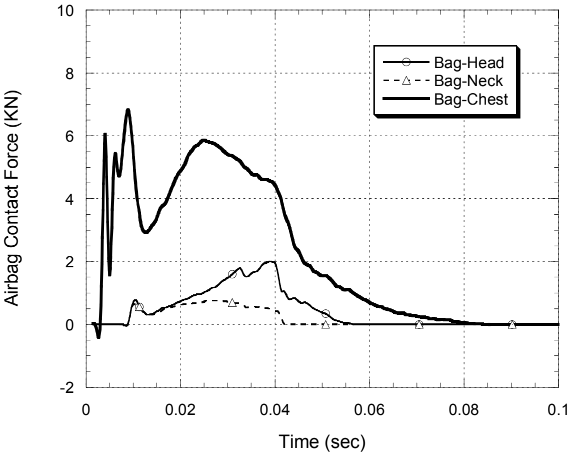

(a) FE contact forces

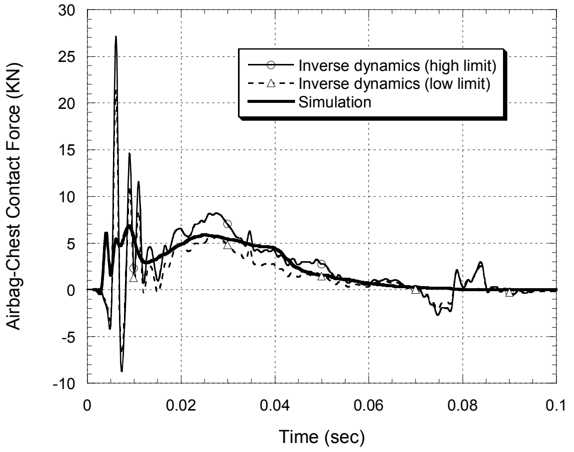

(b) Chest contact load comparison with inverse dynamics

Figure 8: Contact load data comparison.

Neck Load Comparison

Figures 9 and 10 show the data comparison for the upper head/neck shear forces FX, axial forces FZ, and lateral moments My for the ATS tests with bag A. The calculated FZ loads compare fairly well with data, especially in the peak values and timings (Figures 9b and 10b). The model underpredicts the head/neck shear FX fairly significantly (Figures 9a and 10a); but with somewhat better data comparison for My (Figures 9c and 10c). The calculated directions for FX and My agree well with the data, which shows the calculated head flexion/extension trend is consistent with the data (Figures 9 and 10). The neck load data comparison for bag B follows the similar trend as bag A (Figures 11 and 12). It should be noted that the LSTC dummy models were used basically “as is” with no special tuning of the head/neck model parameters.

Bag-Dummy Standoff Effect Simulation

To study the effect of proximity on airbag load from OOP to IP conditions, simulations were carried out with the initial bag-dummy standoff of 25 mm increased to 100 and 250 mm successively (Figure 13). All other parameters were kept the same. Simulations were carried out using bag A with the 5th percentile dummy.

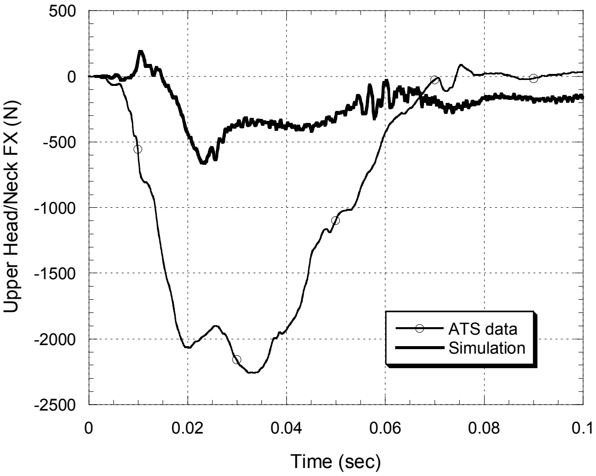

(a) Upper head/neck FX

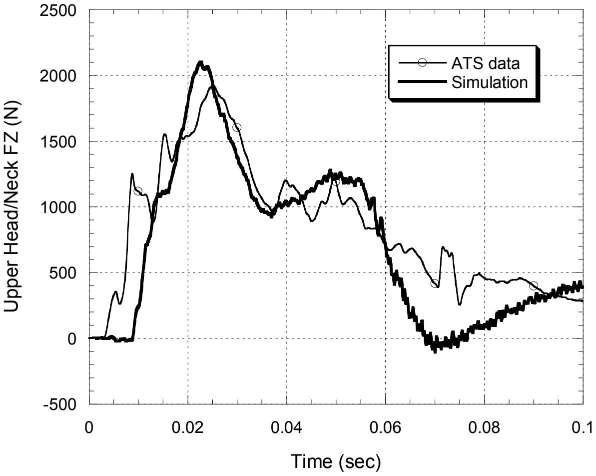

(b) Upper head/neck FZ

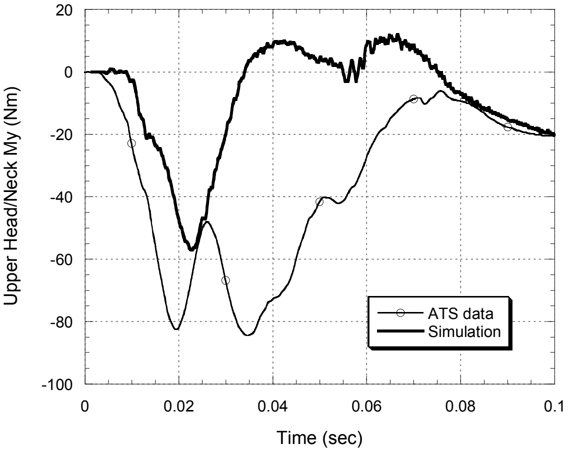

(c) Upper head/neck My

Figure 9: Validation of upper head/neck load: bag A with 5th percentile dummy.

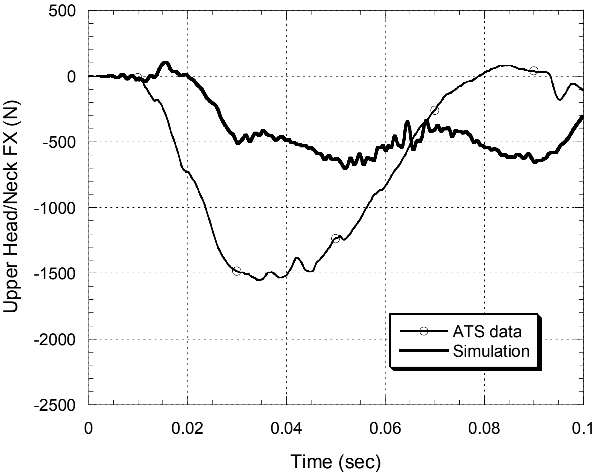

(a) Upper head/neck FX

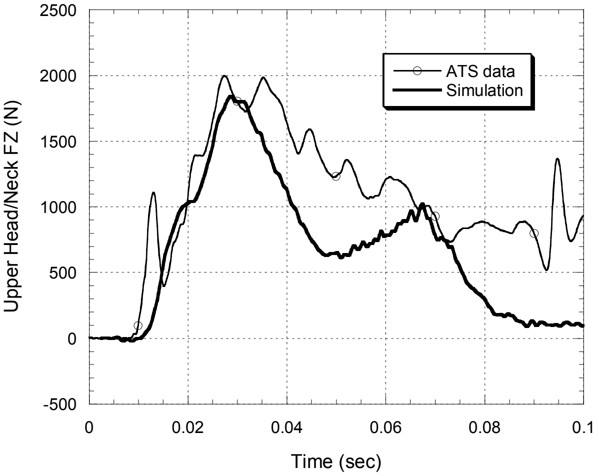

(b) Upper head/neck FZ

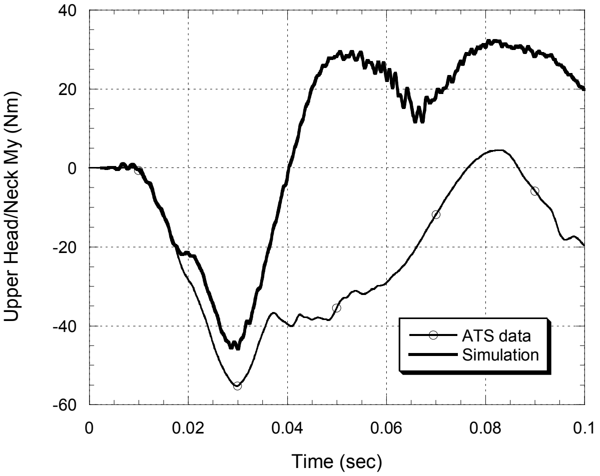

(c) Upper head/neck My

Figure 10: Validation of upper head/neck load: bag A with 50th percentile dummy.

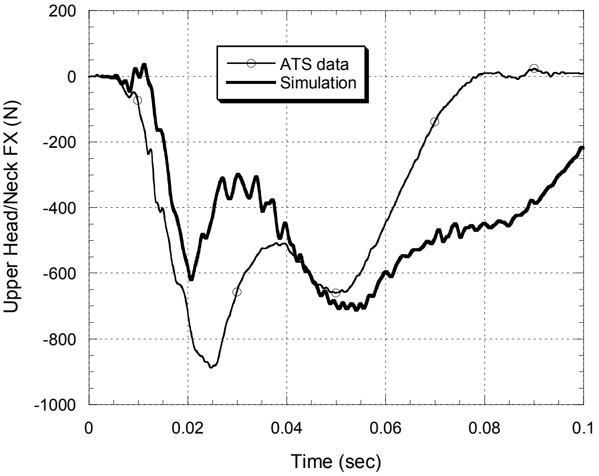

(a) Upper head/neck FX

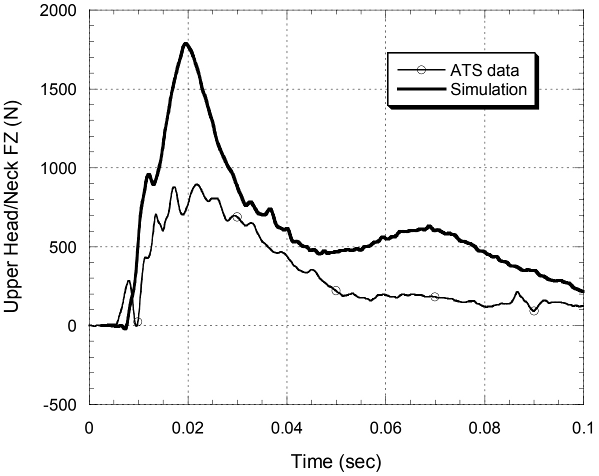

(b) Upper head/neck FZ

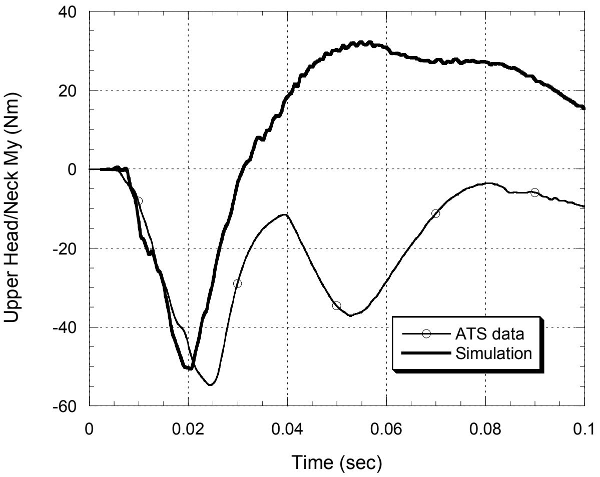

(c) Upper head/neck My

Figure 11: Validation of upper head/neck load: bag B with 5th percentile dummy.

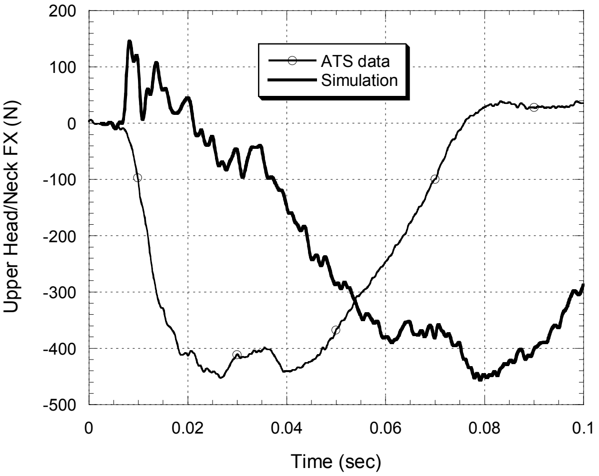

(a) Upper head/neck FX

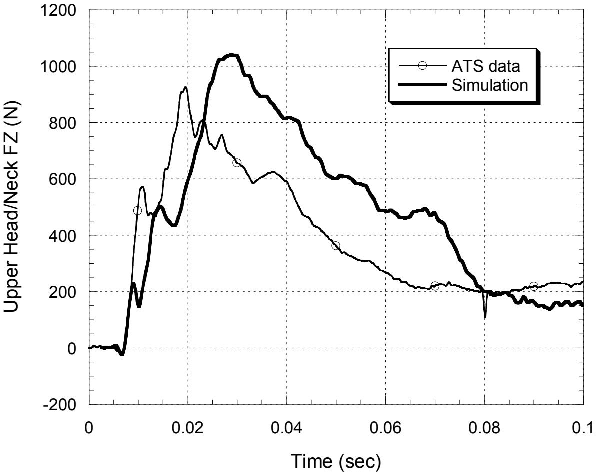

(b) Upper head/neck FZ

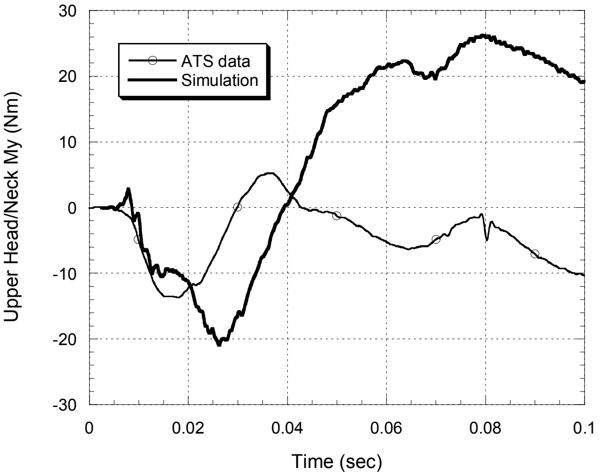

(c) Upper head/neck My

Figure 12: Validation of upper head/neck load: bag B with 50th percentile dummy.

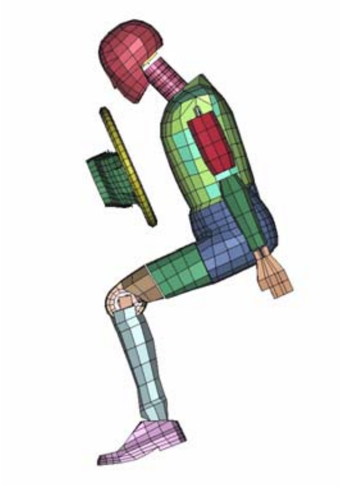

(a) 100 mm standoff

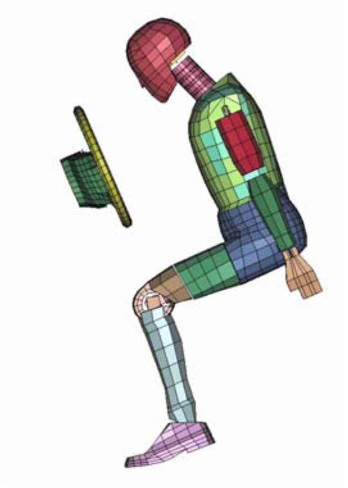

(b) 250 mm standoff

Figure 13: Bag A with 5th percentile dummy at 100 and 250 mm standoffs.

The simulated results show an initial punch-out pressure spike for all three standoffs that characterizes the early inflation phase, with the highest peak and longest duration observed for the 25 mm standoff case (Figure 14a). When the dummy is at the closest standoff of 25 mm, the initial expansion of the bag is hindered not only by the mass of the bag but also the dummy. This leads to stronger bag pressure build up that results in a higher and wider punch out pressure pulse when compared to the cases for 100 and 250 mm standoff. From 20 to 40 ms, simulations show the overall weakening of the airbag pressurization with standoff (Figure 14a). The final pressure peak is 8 psi at 27 ms for the 25 mm standoff, 6 psi at 33 ms for 100 mm standoff, and 4 psi at 40 ms for 250 mm standoff (Figure 14a).

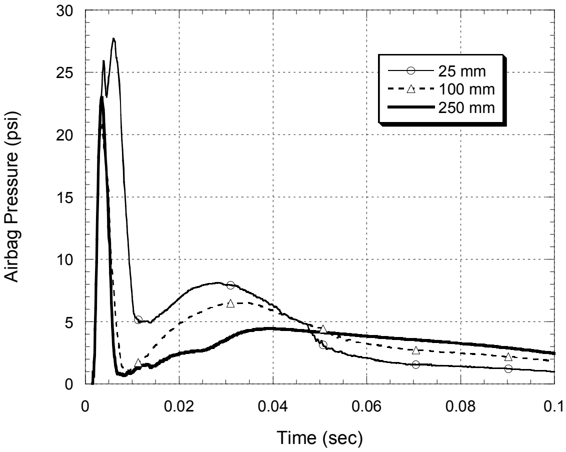

(a) Airbag pressure

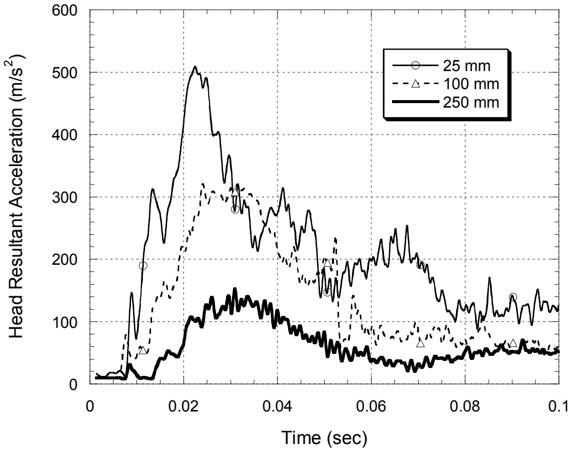

(b) Head acceleration

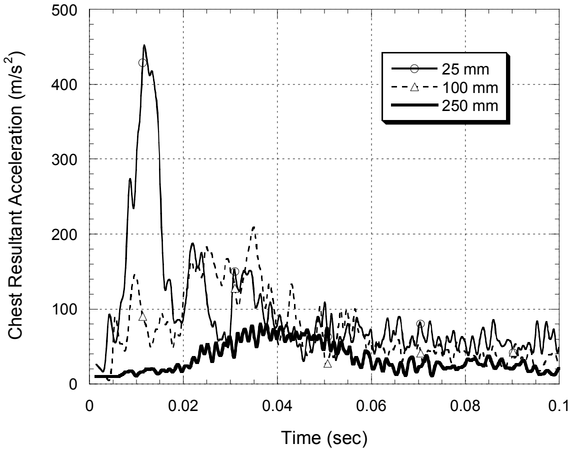

(c) Chest acceleration

Figure 14: Standoff effects on bag A with 5th percentile dummy.

Simulations show that the overall weakening of airbag pressure with standoff correlates with the reduction of dummy head and chest accelerations (Figures 14b-c). When the dummy standoff is increased to 100 mm, the initial punch-out load is much smaller as indicated by the peak chest acceleration of 140 m/s^2 vs. 450 m/s^2 at 10 ms for the 25 mm standoff (Figure 14c). However, during the membrane-loading phase from 20-40 ms, the chest acceleration for the 100 mm case is similar to that for the 25 mm case (Figure 14c). The chest acceleration becomes much smaller with no initial punch-out load when the dummy is moved further to 250 mm (Figure 14c). At 250 mm standoff, the bag barely touches the dummy; hence the bag-dummy contact area is much smaller than that for the 25 or 100 mm cases (Figure 14c). This is consistent with the weakening of the final pressurization process with standoff from 20-60 ms (Figure 14a).

At the ISO-2 position, the airbag mainly contacts with the dummy chest (Figure 1). The dummy head acceleration is mainly due to the chest movement transmitted through the neck. The calculated head accelerations show a general decrease with standoff as expected (Figure 14b). The peak head acceleration decreases from 500 m/s^2 at 25 mm standoff to 120 m/s^2 at 250 mm standoff (Figure 14b).

Crash Test Simulation

The bag A with 5th percentile dummy model was used to simulate airbag-dummy interaction under crash conditions. The dummy was placed at 100 or 250 mm initial standoff from the bag. The crash condition was simulated with the dummy moving towards the bag at an initial velocity with the bag inflation starting at the same time. Note that this dummy relative velocity is not the same as but lower than the crash velocity because in a crash event, most of the energy is absorbed by the vehicle structure deformation rather than the occupant protection system. The acceleration difference between the frame accelerometer and dummy chest accelerometer was obtained by analyzing the NCAP data (NHTSA, 1999). The results suggested a range of relative velocity from 2-6 m/s for typical passenger vehicles under 25-30 mph crash conditions. Calculations were carried out over a range of relative velocity and standoff conditions.

Figure 15 shows the simulation of bag A with the 5th percentile dummy at 100 mm standoff and initial dummy velocity of 4 m/s. At about 21 ms, the dummy comes to rest due to the airbag cushioning effect followed by a rebound indicated by negative velocities (Figures 15b, c and d).

At 100 mm standoff, the effects of increasing the initial dummy velocity from 0 to 4 m/s are shown in Figure 16. The dummy with higher initial velocity will push against the airbag harder, and the peak airbag pressure during membrane-loading phase (20-40 ms) increases from 6 to 9 psi (Figure 16a). Consequently, the higher airbag pressure causes the peak dummy rebound velocity to increase from 4.5 to 5.5 m/s (Figure 16b). The simulations show that if the airbag is compressed more, more energy is transferred to the airbag as shown by the higher bag pressure, and part of that energy will be released back to the dummy.

When the standoff is increased to 250 mm (Figure 17), the membrane airbag pressure peaks at a later time (Figures 16a vs. 17a) as the dummy needs to travel a longer distance to result in a similar airbag compression. Therefore, the peak membrane bag pressure and final dummy rebound (negative) velocity decrease with standoff under crash conditions as expected (Figures 16a vs. 17a, 16b vs. 17b).

DISCUSSION

Finite element model simulations have been performed to study airbag-dummy interactions with validation against ATS data. The airbag unfolding process is well simulated by the model. Good data agreement is observed for airbag pressure and dummy accelerations, while qualitative data agreement is achieved for head/neck loads. Simulation results for the effects of standoff and crash speed on dummy responses are generally considered reasonable.

The validation results show that further refinement of the Hybrid III head/neck model component is needed. The Hybrid III model is used practically “as-is” as provided by LSTC. Based on the favorable data comparison obtained for the dummy kinematics, further improvement of the head/neck load data comparison should be achievable. The effort will likely involve sensitivity studies of the head/neck model parameters and bag contacts with the head and neck.

(a) 5 ms (b) 21 ms

(c) 50 ms (b) 90 ms

Figure 15: Crash simulation at 100 mm standoff with 4 m/s dummy velocity.

The assumption of uniform airbag pressure and temperature seems to have worked fairly well for the present study while some limitations are recognized. It is known that airbag inflation involves a complex turbulent flow with moving boundaries. There is an emerging trend to carry out a full Eulerian-Lagrangian simulation of the airbag-dummy interaction. This requires the solution of the full Navier-Stokes equations for the fluid inside the airbag in an expanding computational boundary coupled with the airbag contact with the moving dummy. This type of modeling is still at a research level with many difficult modeling issues yet to be resolved. Certainly that should be the future of the airbag-occupant model simulation.

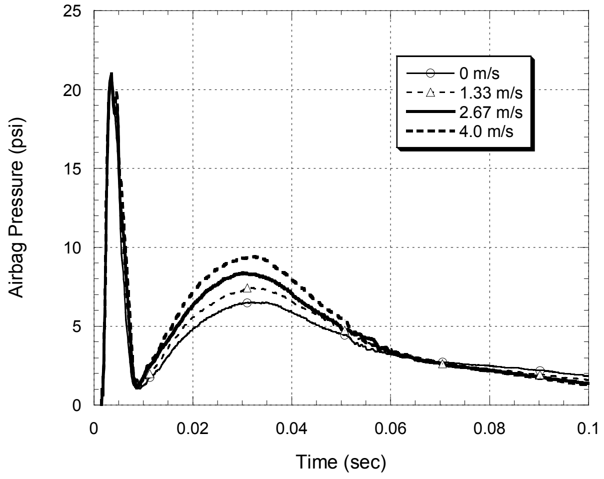

(a) Airbag pressure

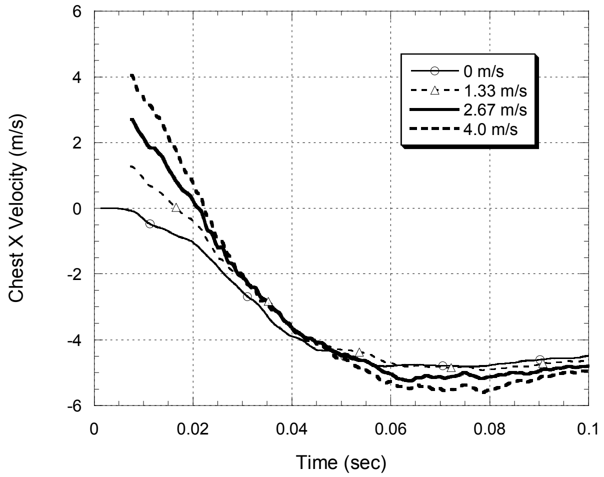

(b) Dummy chest X velocity

Figure 16: Effects of crash velocity on dummy response: bag A with 5th percentile dummy at 100 mm standoff.

The present study has been limited to using only two airbags. The airbag model has performed well for the two selected airbags. The use of the ATS data has provided well defined inflation parameters for the airbag model. The present work also illustrates the importance of having repeatable benchmark data for airbag model validation.

CONCLUSIONS

Finite element airbag-dummy models have been constructed and validated against benchmark test data. The present study shows that a finite element airbag model with a uniform pressure method can give a satisfactory level of validation to capture the key events of the airbag inflation and bag-dummy interaction. Detailed insights of bag-dummy interaction under various standoffs and crash conditions are also identified using model simulations.

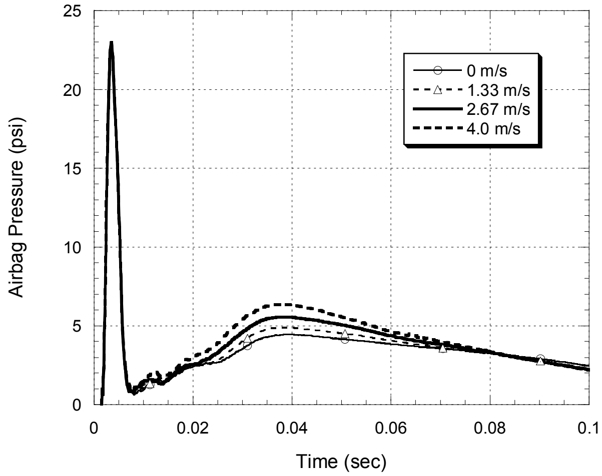

(a) Airbag pressure

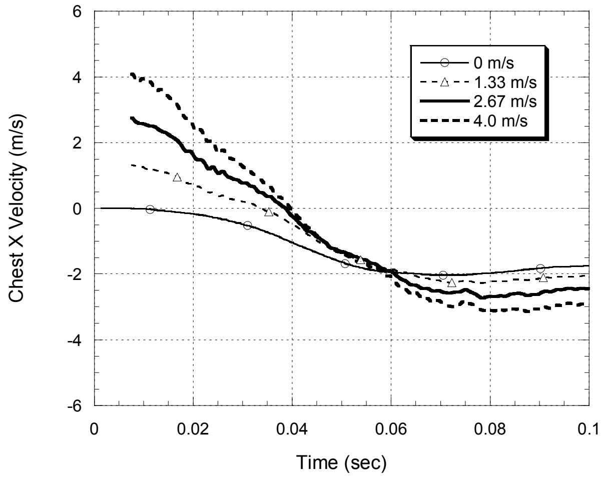

(b) Dummy chest X velocity

Figure 17: Effects of crash velocity on dummy response: bag A with 5th percentile dummy at 250 mm standoff.

ACKNOWLEDGEMENTS

This work has been sponsored by the National Highway Transportation and Safety Administration (NHTSA), under a Joint Cooperative Research Agreement with the US Army Medical Research and Material Command (MRMC). The authors appreciate the support and encouragement of Drs. Rolf Eppinger and Erik Takhounts during the course of this study. The authors are responsible for all statements and opinions expressed.

REFERENCES

BANDAK, F., CHAN, P. C., HO, K. H., and LU, Z. (2002). An Experimental Air Bag Test System for the Study of Air Bag Deployment Loads. Int. J. Crashworthiness, 7(2), pp.1-12.

DIGGIES, K., NOUREDDLINE, A., and BEDEWI, N. E. (1997). Chest Injury Risks to Drivers for Alternative Air Bag Inflation Rates. SAE Paper 970129, Occupant Protection and Injury Assessment in the Automotive Crash Environment, SAE SP-1231.

JOHNSTON, K. L., KLINICH, K. D., RHULE, D. A., and SAUL, R. A. (1997). Assessing arm injury potential from deploying air bag. SAE Paper 970400, Occupant Protection and Injury Assessment in the Automotive Crash Environment. SP-1231.

LAU, I. V., HORSCH, J. D., VIANO, D. C., et al., (1993). Mechanism of injury from air bag deployment loads. Accid. Anal. Prev. 25, 29.

LIN, T.-C., WAWA, C., and KHALIL, T. B. (1995). Evaluation of the Hybrid III Dummy Interactions with Air Bag in Frontal Crash by Finite Element Simulation. SAE Paper 952705, 37th Stapp Car Crash Conference Proceedings, SAE P-299.

LU, Z. and CHAN, P. C. (2003). Airbag Test Simulator (ATS) Calibration and Parametric Studies Using Simple Targets. Jaycor Technical Report J2997.102-03-189, Contract No. DAMD17-96-C-6007, January 2003.

LU, Z. and CHAN, P. C. (2005). Finite Element Simulation Study of Airbag Load Phenomena. SAE Paper 2005-01-0301.

NHTSA (1999). NCAP data, 1996-1999.

NHTSA (2000). FMVSS, 49 CFR 571. 208.

O'CONNOR, C. S., and RAO, M. K. (1992). Development of a Model of a Three-Year-Old Child Dummy Used in Air Bag Applications. SAE Paper 922517, 36th Stapp Car Crash Conference Proceedings, SAE P-261.

PATRICK, L. and NYQUIST, G., (1972). Air Bag Effects on the Out-of-Position Child. Second International Conference on Passive Restraints, SAE Paper 720442, Biomechanics of Impact Injuries and Injury Tolerances of the Abdomen, Lumbar Spine and Pelvis Complex. edited by S. Backaitis, (SAE, 1995).

PETIT, P., TROSSEILLE, X., BAUDRIT, P., and GOPAL, M. (2003). Finite Element Simulation Study of a Frontal Driver Airbag Deployment for Out-of-Position Situations. 47th Stapp Car Crash Conference Proceedings, P-385.

PLANK, G. R., KLEINBERGER, M., and EPPINGER, R. H. (1998). Analytical Investigation of Drive Thoracic Response to Out of Position Airbag Deployment. SAE Paper 983165, 42nd Stapp Car Crash Conference Proceedings, SAE P-337.

RUAN, J. S. and PRASAD, P. (1994). Head Injury Potential Assessment in Frontal Impacts by Mathematical Modeling. SAE paper 942212, 38th Stapp Car Crash Conference Proceedings, SAE P-279.

SAE J2238 (1995). Airbag Inflator Ballistic Tank Test Procedure. SAE Surface Vehicle Recommended Practice, March 1995.

SEEMANN, M.R., MUZZY, W.H., and LUSTICK, L.S. (1986). Comparison of Human and Hybrid III Head and Neck Dynamics Response. Proc. of the 30th Stapp Car Crash Conf., SAE Paper 861892.

SIEVEKA. E., CRANDALL, J., DUMA, S., and PIKEY, W. (1999). Three Year Old Child and Side Airbag Interaction Study Using the CVS/ATB Multi-body Simulation Program. SAE Paper 1999-01-0756, in Air Bag Technology, SAE SP-1411.

TANAVDE, A. S., GUDIPATY, K., and VALDYARAMAN, S. (1997). Simulation of Seat Integrated Side Airbag Deployment. SAE Paper 970127, Occupant Protection and Injury Assessment in the Automotive Crash Environment, SAE SP-1231.

VAIDYARAMAN, S., KLANDELWAL, H., LEE, C., XU, J., and NAYEF, A. (1998). State-of-the-art side airbag modeling and its application in occupant safety in lateral collisions. SAE Paper 980915, in Airbag Technology, SAE SP-1333.

YOGANANDAN, N., PINTAR, F. A., SKRADE, D., CHMIEL, W., REINARTZ, J. M., and SANCES, A., JR. (1993). Thoracic Biomechanics with Air Bag Restraint. SAE Paper 933121, 37th Stapp Car Crash Conference Proceedings, P-269.

WAWA, C. J., CHANDRA, J. S., and VERMA, M. K (1993). Implementation and validation of a finite element approach to simulate occupant crashes with airbags: Part I – airbag model. in Crashworthiness and occupant protection in transportation systems. AMD-Vol. 169/BED-Vol. 25 (ASME, 1993).

DISCUSSION

PAPER: **Finite Element Model Simulation of Airbag-Dummy Interaction**

PRESENTER: ***Zi Lu, Titan Corporation***

QUESTION: *Guy Nusholtz, Daimler Chrysler*
Couple technical things: The last time I used LS-DYNA for simulation, which was a couple years ago, I couldn't get the energy to balance. In other words, more energy came out of the system than you put into it.

ANSWER: Yeah. This one, I also noticed that. Actually, I checked. In any event, it's only 5 to 10% difference so no big difference.

Q: Well, in some cases it can be as much as 20%.

A: Oh, okay.

Q: Somehow it creates energy in the process.

A: Yeah, I know. I know.

Q: So, okay. That answers the question. It's still there. There are some simulations, which I've done, which have been as much as 30%. Most of the time, it runs between 5—basically between 2% and 10%.

A: Ten percent.

Q: But every once in a while, you get more energy.

A: Yeah, especially for the airbag simulation, I've seen.

Q: The other question is: In some of your simulations, you had a rather sharp drop-off in the time histories. Do you know why that is? I mean, things, which were not physically—Let's see if we can find one. There's one.

A: You mean in this one?

Q: Yeah.

A: Yeah. Actually, this one. We take LSTC dummy model. Actually, we just change the sound and the value against MBT slat. We think we still need much improvement in the dummy model.

Q: Okay. So that's a dummy model.

A: Dummy model. Also, this one is very sensitive. Actually, we changed the position a little bit. Maybe some of this one goes our way or maybe up here in other position here sometimes happens.

Q: Okay. So there's still some stuff that [we] have to deal with dummy models.

A: Actually, dummy model—We need to improve it actually.

Q: And I guess the basic conclusion from your research is: You don't really need to do all that complex CFD. You can pretty much do an out-of-position simulation over one parameter because that's what you're using, right?

A: Yeah. Actually, for this one we—but this one you need to be careful. We use as increment one step of the airbag model. You need to control a lot of details. You need to control your readings, folding the airbag. Also, and you need control—Also, you need an element very small. In terms of the airbag, the element is small. Also you need a variety of the input of the mass flow rate to that one. Also, for hour go to this stage, go to calibration against the cylindrical target. We calibrated the airbag among the first. Before the first, we try to use the airbag with dummy, you have a lot of parameters and you have diameter. You can change airbag. Finally, you don't know what to change so we just go one step at a time. I think right now it's a reasonable result.

Q: It's a tuning process because you don't exactly know what is the correct parameters to put in. You just know the results are good.

A: Oh no. Actually because our simulation here—We calibrated the airbag here with cylindrical target. For cylindrical target, match the dimension, match the mass flow and the moment of inertia. Here, too, the airbag model calibrator. We just cut off this airbag and don't change elastic and come integrated with the habistrate [?] model. In terms of kinematic, it's pretty good right now, but I would still other work to do, like panetra mode, something obscure has—

Q: Just a short question: You said you had to get the mass flow correct. Was it important to get the temperature or did that not matter?

A: For our eight years tests, here because we used pressurized air, temperature is room temperature. But during a test, because it's a fast gas expansion, the temperature could drop 50 or 60° like a refrigerator. The initial, the temperature here is room temperature. For effrata (?) test—We also conducted the effrata (?) test with a model of temperature. We saw the similar dynamics equation also can get mass flow rate at a zeta temperature, like 600 or 700 k for typical inflated time test.

Q: Thank you.

Q: *King Yang, Wayne State University*
I'd like to congratulate you on this very tedious work for airbag. I'm impressed. Some 10 years ago, we tried that and published a couple of, Stapp papers and we stopped doing that because most of the accidents you see in your life, the driver was actually turning the wheel. So all the time you spend floating the airbag and then test it in one position, by the time you twist that airbag to a different angle, the dynamics change. So we start doing that. I'd just like to hear your comments.

A: Also from our test, from our simulation, you change the body position or the dummy position or you change the air bag a little bit, you can get a different result. But the reason our developed our airbag model here, because we have eight test assistants who test it and we get a lot of repeatable tests. You fix the position of dummy on here. From here, we have some position of the arm to fist down, you can get a very repeatable dummy response, which also—we have those tests and we have developed a model to help us to understand the test data.